JOURNAL OF CATALYSIS 56, 21–31 (1979)

Effects of the Surface Structure of Rh/γ-Al_2O_3 on the Hydrogenolysis of *n*-Pentane, on the Oxidation of *n*-Butane, and on the Reduction of Nitric Oxide

H. C. YAO, Y.-F. YU YAO, AND K. OTTO

Engineering and Research Staff, Ford Motor Company, Dearborn, Michigan 48121

Received April 6, 1978; revised August 2, 1978

In low-concentration Rh catalysts, supported on γ-Al_2O_3, the metal is present in a dispersed phase with every Rh atom or ion exposed on the surface. This form persists up to a surface concentration of 2.5 μmol/m^2 (BET). At higher concentrations three-dimensional particles are formed. Three model reactions were investigated on Rh catalysts of both kinds: hydrogenolysis of *n*-pentane under strongly reducing conditions, oxidation of *n*-butane under strongly oxidizing conditions, and reduction of nitric oxide by hydrogen under mildly oxidizing conditions. The *n*-butane oxidation proceeded in the same fashion on both types of Rh catalysts, while the two other reactions were found to be structure sensitive. On the dispersed phase, *n*-pentane cleaves predominantly into ethane and propane, while on the three-dimensional particles this activity is sharply diminished. Similarly, the product selectivity and the kinetic parameters of the NO–H_2 reaction differ distinctly on the two phases of supported Rh.

INTRODUCTION

Several transition metal oxides can be deposited on insulator supports, such as alumina or zirconia, to form a well-dispersed phase, δ-phase (*1–7*). The surface concentration of the metal ions increases with metal loading until saturation of the δ-phase is reached (*4–7*). Beyond this concentration, excess transition-metal oxide forms clusters or crystallites on the support (β-phase). The saturation concentration of the δ-phase varies with the transition-metal oxide and also with the support material (*4–6*).

For Rh^{3+} on γ-alumina, a saturation concentration of 2.5 μmol/m^2 (BET) was measured by chemisorption (*6*), which covers only about 10% of the support area, assuming that the Rh is closely packed in two-dimensional patches. Although metal ions in the δ-phase are stable at high temperatures, for example, Co^{2+} on ZrO_2 at 800°C (*7*), it is not certain that metal ions can always remain dispersed after reduction at high temperatures. Recently, evidence was found (*8*) that well-dispersed Rh^{3+} in the δ-phase can remain atomically dispersed after reduction in H_2 to Rh^0 at 400°C.

Conventional methods, such as chemisorption, electron microscopy, or X-ray diffraction cannot easily discriminate between two-dimensional patches of reduced metal and small crystallites if the particle size is less than 20 Å.

To distinguish between these two phases one can employ a structure-sentitive catalytic reaction. Thus, Corolleur *et al.* (*9, 10*) compared the hydrogenolysis of methyl pentane and *n*-hexane over different concentrations of Pt on Al_2O_3. They found a wide variation of the product dis-

0021-9517/79/010021-11$02.00/0

tribution with metal concentration. Particle size also affects activity and product distribution in the NH_3 oxidation on Al_2O_3-supported Pt (*11–13*). Boudart *et al.* (*14*) found that the rate ratio of neopentane isomerization and hydrogenolysis on supported Pt at various dispersions changed by a factor of 100. Yates and Sinfelt (*15*) studied the catalytic activity of Rh, supported on silica, for ethane hydrogenolysis and observed a distinct dependence on particle size. They suggested that the highest activity was associated with an intermediate degree of dispersion.

To explore the differences in catalytic behavior between the metal oxide phases, δ and β, and the metallic phases derived from these by reduction, we have employed a series of Rh catalysts supported on γ-alumina, which had been characterized by chemisorption of different adsorbates (*6*). Catalyst activity and selectivity were measured as a function of Rh concentration. Three model reactions were selected: hydrogenolysis of *n*-pentane, oxidation of *n*-butane, and reduction of nitric oxide by hydrogen.

EXPERIMENTAL

I. Catalyst Preparation

The preparation and characterization of the Rh/γ-Al_2O_3 catalysts used for this study have been reported elsewhere (*6*). All the catalysts used during this study were calcined in air at 500°C for at least 2 hr. Only the catalysts used in the hydrogenolysis of *n*-pentane were prereduced by hydrogen at 400°C. The saturation concentration of Rh in the δ-phase was measured by the chemisorption of NO, CO, and H_2 (*6*). The BET surface area of the γ-alumina employed was about 150 m^2/g.

II. Rate Measurements

A. Hydrogenolysis of n-pentane. The hydrogenolysis rates were measured in a batch reactor equipped with a reciprocating pump and a pressure transducer. Product analyses were performed using a gas chromatograph. Details of the experimental technique have been reported by Dalla Betta *et al.* (*16*).

B. Oxidation of n-butane by oxygen. Because of the highly exothermic nature of this reaction, a flow reactor was preferred. Details of the experimental technique have been reported (*17*). The concentrations of reactants and products were analyzed with a mass spectrometer connected to the reactor. The ratio of oxygen to *n*-butane in a carrier gas, He, was usually kept considerably above the stoichiometric ratio. The catalyst temperature was controlled to within ±2°C and continuously monitored with a recorder. For the rate measurements, precautions were taken to avoid thermal and mass-transport influences by selecting proper flow rates and sample sizes. In all cases, the *n*-butane concentration was kept below 0.2%, and the conversion, below 30%. Prior to each run, the sample was heated to 500°C in a stream of helium containing about 1% oxygen to remove water and other surface contaminants. The material balance of carbon showed that *n*-butane was stoichiometrically converted to CO_2; therefore the rate of CO_2 formation was taken as a measurement of the rate of *n*-butane oxidation. The oxidation rate readily attained a constant value after each change in the inlet composition or the reaction temperature. No induction period or decay was observed over the duration of the experiments, 2 to 6 hr.

C. Reduction of NO by H_2. A batch reactor, similar to that in the hydrogenolysis study, was used for investigating the reduction of NO by hydrogen. At the beginning of each experiment, the recirculation system was filled with a mixture of 42 Torr NO, 37 Torr H_2, and 180 Torr Ar as a carrier gas. The sample sizes were chosen so that each catalyst charge exposed approximately the same number of

Rh surface atoms, as measured by the chemisorption of NO, CO, and H_2. Reaction temperatures were selected in the range from 60 to 200°C. During the reaction, small samples of the gas mixture were injected into a mass spectrometer to measure the concentrations of NO, N_2O, and N_2. The reduction of nitric oxide to ammonia was determined by difference from the nitrogen mass balance. Further details of the experimental setup have been given previously (*18*).

RESULTS

I. Hydrogenolysis of n-Pentane

A. Rate measurements. Hydrogenolysis of *n*-pentane was examined over six samples of various Rh concentrations. Two examples of such measurements as a function of time are given in Fig. 1. They show the reaction products over a dilute and over a concentrated Rh catalyst. Although all reactions produce methane, ethane, propane, and *n*-butane, the relative partial pressures of the hydrocarbons produced vary with the Rh concentration. For catalysts with low Rh concentrations, the reaction produces relatively high concentrations of ethane and propane, but low concentrations of methane and *n*-butane, This difference decreases as the Rh concentration increases, and eventually the partial pressures of methane and *n*-butane become higher than those of ethane and propane (Fig. 1B). In all cases, the amounts of isopentane and isobutane are very small, i.e., the isomerization reaction is negligible.

B. Rate dependence on Rh loading. The initial rates of *n*-pentane hydrogenolysis (r_0), ethane formation (r_1), and *n*-butane formation (r_2) at 100°C are given in Table

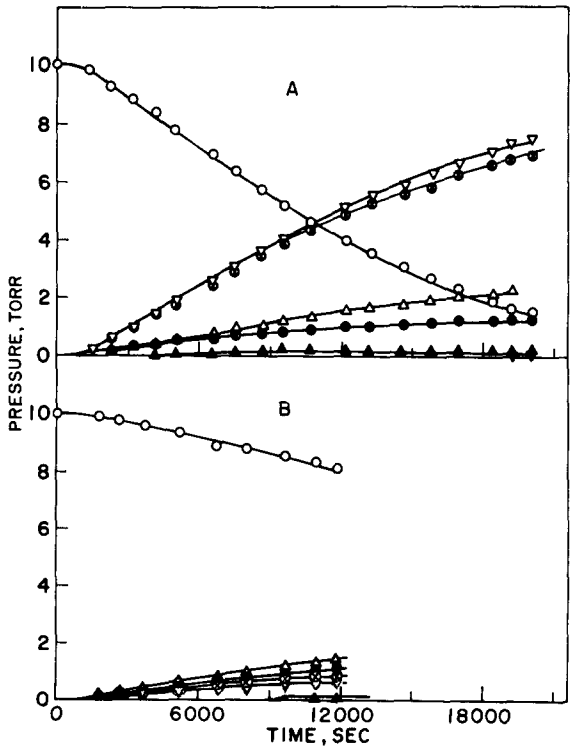

FIG. 1. Hydrogenolysis of *n*-pentane at 100°C over (A, top) 1.89 wt% Rh, 0.68 g; (B, bottom) 12.40 wt% Rh, 0.37 g. (○) *n*-Pentane, (△) methane, (▽) ethane, (⊗) propane, (●) *n*-butane, (▲) isopentane, (▼) isobutane.

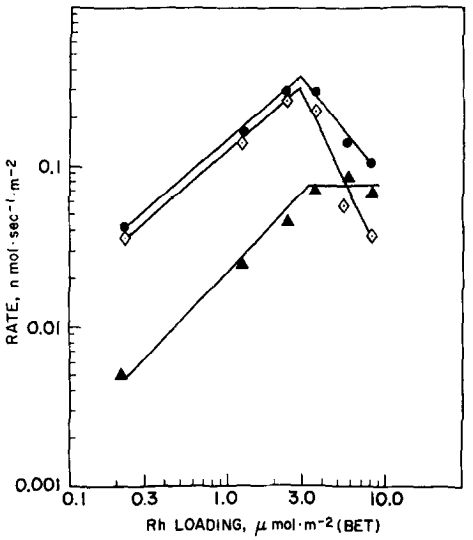

FIG. 2. Initial rates of *n*-pentane hydrogenolysis (●) r_0, ethane formation (◇) r_1, and *n*-butane formation (▲) r_2 at 100°C.

1, and their dependence on the Rh loading is plotted in Fig. 2. Each logarithmic plot of the initial rate versus Rh loading consists of two approximately linear sections. In the segments of low Rh loading, r_0, r_1, and r_2 increase with increasing Rh loading up to about 2.8 μmol/m² (BET). Beyond this concentration, r_0 and r_1 decrease, while r_2 levels off. The turnover numbers, *T.N.*, of these reactions are compared in Table 1. It is assumed that the Rh in samples with concentrations of less than about 2.5 μmol/m² (BET) is completely exposed on the surface of γ-alumina because a concentration of about 2.5 μmol/m² is the saturated concentration of the δ-phase before reduction (*6*). The results in Table 1 show parallel changes of $(T.N.)_0$ and $(T.N.)_1$. They show a smaller decline in turnover number with Rh loading in the dispersed phase and a steeper decline in the particulate phase. On the other hand, the turnover number for the formation of *n*-butane remains fairly constant for both the dispersed and particulate phases.

II. Oxidation of n-Butane

A. Kinetic parameters. The effect of the partial pressures of O_2 and *n*-C_4H_{10} on the oxidation rates was determined by a method described previously (*17*). The reaction orders with respect to *n*-C_4H_{10} and O_2 are 0.2 and 0.1, respectively. This was found true for catalysts of low and high Rh content. The apparent activation energies and the reaction rates at 300°C are listed in Table 2.

B. Rate dependence on Rh loading. The rates of *n*-C_4H_{10} oxidation are shown in Fig. 3. The logarithmic plot of the rate, expressed in nanomoles (10^{-9} mol) of CO_2 formed per second per square meter (BET) versus the Rh loading, in micromoles of Rh per square meter (BET), con-

TABLE 1

Initial Rates for *n*-Pentane Hydrogenolysis[a]

Rh loading		Rate at 100°C (nmol m⁻² sec⁻¹)			Turnover number (ksec⁻¹)		
(wt%)	(μmol m⁻²)	r_0	r_1	r_2	$(T.N.)_0$	$(T.N.)_1$	$(T.N.)_2$
0.34	0.22	0.042	0.037	0.005	0.190	0.168	0.023
1.89	1.22	0.168	0.143	0.025	0.138	0.118	0.020
3.66	2.36	0.303	0.257	0.046	0.128	0.108	0.020
5.51	3.55[b]	0.297	0.225	0.072	0.118	0.090	0.028
8.71	5.62[b]	0.145	0.058	0.087	0.058	0.023	0.034
12.40	8.00[b]	0.107	0.038	0.069	0.043	0.015	0.028

[a] Initial pressures: $P(n\text{-}C_5H_{12})$ = 10 Torr, $P(H_2)$ = 100 Torr.
[b] Saturation concentration of surface Rh is 2.5 μmol m⁻² (*6*).

sists of two linear sections. On the catalysts of low Rh loading, the oxidation rate increases with increasing Rh concentration up to about 2.4 μmol of Rh/m^2 (BET) beyond which the rate levels off. The turnover number (Table 2), which measures the average activity of each surface Rh atom, remains fairly constant (within 25% of the average value).

III. Reduction of Nitric Oxide by Hydrogen

A. Rate measurements. The rates of reduction of NO by H_2 were measured on four of the Rh catalysts. An example of the components of the reaction mixture as a function of time is given in Fig. 4.

Reaction rates were evaluated at the point where 50% of the initial amount of NO had been reduced. In Table 3, these rates are listed for a reaction temperature of 100°C, together with turnover numbers and apparent activation energies. The reduction of NO by hydrogen over a bare surface of γ-alumina was too slow to be measured, even at 300°C.

B. Rate dependence on Rh loading. Although the rate of NO reduction increases with the Rh loading over the whole Rh loading range, this increase is sharpest at the highest loading, in contrast to the results of hydrogenolysis and oxidation. A logarithmic plot of the rates as a function of Rh loading is given in Fig. 5, showing the abrupt change at about 2.8 μmol/m^2.

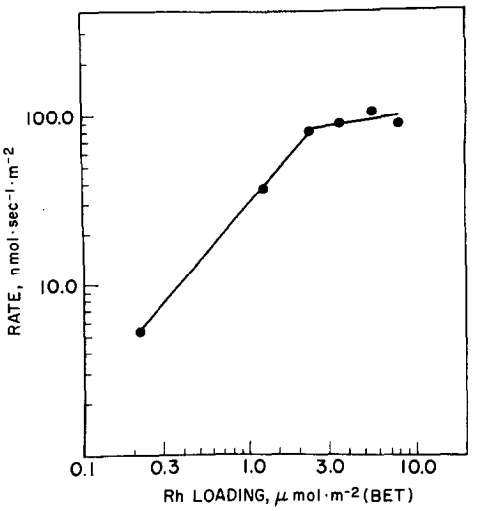

FIG. 3. Rates of *n*-butane oxidation at 300°C (steady state).

DISCUSSION

A comparison of the results obtained for the three reactions studied here shows certain similar trends of the dependence on Rh concentration in the range of the dispersed phase, on the one hand, and distinct differences in the range where the particulate phase prevails, on the other hand. For example, the rate increase of each of the three reactions is linear with the Rh

TABLE 2

Reaction Parameters for *n*-Butane Oxidation

Rh loading (wt%)	Rh loading (μmol m^{-2})	Rate at 300°C (nmol m^{-2} sec^{-1})	*T.N.* (ksec^{-1})	Activation energy[a] (kcal mol^{-1})
0.34	0.22	5.4	24.5	24.2
1.89	1.22	38.0	31.1	24.6
3.66	2.36	81.8	34.7	—
5.51	3.55[b]	89.3	35.7	24.1
8.71	5.62[b]	104.1	41.6	23.5
12.40	8.00[b]	89.3	35.7	—

[a] Measured in the range from 250 to 400°C.

[b] Saturation concentration of surface Rh is 2.5 μmol m^{-2} (*6*).

loading in the dilute range, while in the concentrated range the rate of *n*-pentane hydrogenolysis decreases, the rate of *n*-butane oxidation remains constant, and the rate of nitric oxide reduction by hydrogen increases with Rh concentration.

The observed differences in the reaction parameters and the product distributions, which are presumably manifestations of a change in the reaction mechanism, will be discussed first.

I. Hydrogenolysis of n-Pentane

The previous study of *n*-pentane hydrogenolysis over $Rh/\gamma\text{-}Al_2O_3$ catalysts indicated that this reaction takes place through two reaction intermediates (*19*). One is the 2,2,4-triadsorbed intermediate, which dissociates to form only ethane and propane, Eq. 1; the other one is the 1,1,3-triadsorbed intermediate, which dissociates to form either methane and *n*-butane or ethane and propane, Eq. (2).

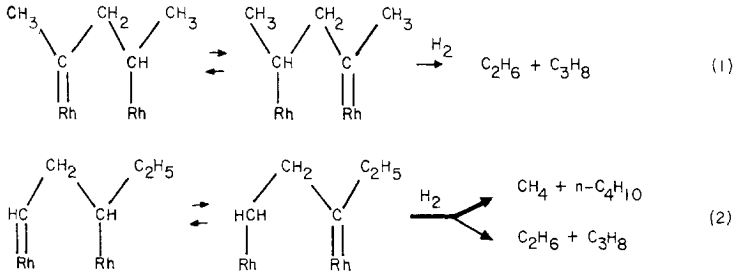

In the dissociation of the 1,1,3-triadsorbed intermediate [Eq. (2)], the formation of methane and *n*-butane is governed by an apparent activation energy which is about 10 kcal/mol lower than that associated with the formation of ethane and propane (*19*). Similarly, over Pt, hydrocracking of a C_I–C_{II} bond (C_I, primary carbon; C_{II}, secondary carbon) was found to be much easier than that of a C_{II}–C_{II} bond (*20*). These facts support the concept that the major products in the dissociation of the 1,1,3-adsorption complex should be methane and *n*-butane, as indicated in Eq. (2) by the reaction path marked with the heavy arrow. Since ethane and propane are the major products over supported Rh in the dispersed phase, it appears that they are derived mainly from the 2,2,4-adsorption mode.

TABLE 3

Reaction Parameters for Nitric Oxide Reduction[a]

Rh loading (wt%)	Rh loading (μmol m^{-2})	Rate at 100°C (nmol m^{-2} sec^{-1})	*T.N.* (ksec^{-1})	Activation energy[b] (kcal mol^{-1})	$N_2/(N_2 + N_2O)$
0.34	0.22	0.048	0.216	14.7	0.11
1.89	1.22	0.218	0.179	14.6	0.08
5.51	3.55[c]	0.65	0.260	9.9	0.10
12.40	8.00[c]	2.90	1.16	8.8	0.45

[a] Initial pressures: $P(NO) = 42$ Torr, $P(H_2) = 37$ Torr.
[b] Measured in the range from 60 to 200°C.
[c] Saturation concentration of surface Rh is 2.5 μmol m^{-2} (*6*).

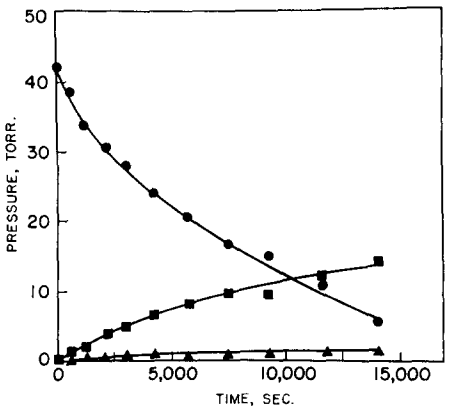

FIG. 4. Reduction of NO by H_2 at 100°C over 5.5 wt% Rh. (●) NO, (▲) N_2, (■) N_2O.

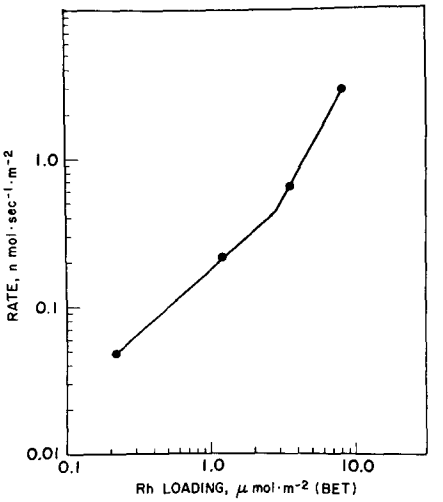

FIG. 5. Reduction rates of NO at 100°C (at 50% conversion).

At higher Rh concentrations the predominant products are CH_4 and n-C_4H_{10} which indicate that here the 1,1,3-adsorption mode is the preferred and possibly only surface intermediate.

The reason for the presence of different reaction intermediates on the two Rh phases is not clear. Since Al_2O_3 by itself is a hydrogenolysis catalyst of low activity (*21*), and since the presence of Al_2O_3 can increase the hydrogenolysis activity of a metal (*22*), one can speculate that the support influences the configuration of the adsorption sites on dispersed Rh so that 2,2,4-triadsorbed intermediates predominate.

The product distribution as a function of Rh concentration on the dispersed phase is distinctly different from that on the particulate phase. For example, a tenfold increase of Rh from 0.22 to 2.36 μmol/m^2 caused the ethane/butane rate ratio to decrease by only 20 to 25% (Table 1). On the other hand, a concentration increase from 3.5 to 5.6 μmol/m^2 resulted in a fivefold decrease of the ratio. The pronounced change in the product distribution at an Rh concentration higher than 2.5 μmol/m^2 is evidence for the formation of many small β-phase crystallites or clusters at the expense of the dispersed phase and indicates that, once the particles start forming, the number of 2,2,4-triadsorbed intermediates decreases sharply, causing a rapid change in the product distribution. The rates and turnover number values given in the tables are the average values of Rh sites in these two phases. When the Rh loading exceeds 2.5 μmol/m^2 (BET), the total number of Rh sites remains essentially constant (*6*) but the ratio of Rh sites in the β-phase to those in the δ-phase increases with increasing Rh loading. From comparison of the rate of ethane formation at 0.22 wt % Rh (all in the δ-phase) in the 12.4 wt% Rh sample, it follows that at 12.4 wt% Rh less than 10% of the total sites exist in the δ-phase.

II. Oxidation of n-Butane by O_2

The results indicate that this reaction, which takes place under oxidizing conditions, is not structure sensitive. Thus, the turnover number and the apparent activation energy remain practically constant as the Rh on the surface, presumably present here in its oxidized form, changes from δ- to β-phase (Table 2). The low apparent reaction orders of n-butane and oxygen of 0.2 and 0.1, respectively, suggest that the rate-determining step occurs on the sur-

face. This assumption requires the reaction rates to be proportional to the number of *n*-butane molecules which are chemisorbed on a presumably oxidized Rh surface (*23*). It is probable that the sites which can accommodate chemisorbed molecules of *n*-butane correspond to those sites which are occupied during the chemisorption of NO, CO, and H_2 (*6*).

III. Reduction of NO by H_2

Values of kinetic parameters for this reaction, carried out close to stoichiometric conditions, are given in Table 3. The four samples which were employed are listed in the order of increasing Rh concentration. The turnover numbers of the samples with the two lowest Rh loadings are identical within experimental error, while the turnover number for the highest Rh loading is fivefold larger. The increase in turnover number is associated with a decrease in the apparent activation energy by 6 kcal/mol. Is it reasonable to assume that the reaction mechanism remains the same, while the activation energy decreases from 15 kcal/mol on the dispersed-phase Rh to 9 kcal/mol on the larger Rh particles? At 100°C such a decrease in the activation energy should result in a rate increase of three orders of magnitude, which disagrees with the measured turnover number, under the assumption that the reaction-site density has remained constant. Consequently, only a very small fraction of surface atoms exposed on the three-dimensional Rh particles could be considered as sites of the higher catalytic activity.

It is more probable that a change in the reaction mechanism is responsible for the observed activity change, which is also suggested by the pronounced increase of the N_2/N_2O ratio at the highest Rh loading and a similar change in the formation of ammonia. Ammonia, which was determined indirectly from the balance of NO, N_2O, and N_2, was found to be below 10%, up to a Rh loading of 5.5 wt%, and it was 25% at the highest Rh loading.

At this juncture it should be pointed out that, during the reduction of nitric oxide by hydrogen, or ammonia, over catalysts containing Pt (*18*), Cu (*24*), or Ru (*25*), the N_2/N_2O ratio is rather unaffected by the concentrations of the reactants or by the temperature, provided the temperature is sufficiently low. It is typical for these reactions that a subsequent reduction of N_2O from the gas phase by hydrogen, or ammonia, is very slow compared to the reduction of NO, as long as an appreciable concentration of NO is present. In the absence of NO, the reduction of N_2O proceeds much faster (*18*, *24*, *25*). The same observations apply for the reduction of NO by H_2 over Rh.

Using a calculation proposed by Maatman (*26*), it is possible to provide further evidence that the slow step in the catalytic reduction of NO by H_2 undergoes a change, as the Rh concentration increases. In this approach, a site density is calculated from basic principles involving partition functions and gas-phase concentrations of the reactants, the specific reaction rate, the apparent activation energy, and universal constants. This calculated density of reaction sites is compared with the geometrically possible site density.

Maatman (*26*) distinguishes five cases for his calculations, based on different reaction mechanisms. The assumptions underlying two of these cases are obviously not applicable to the reduction of NO by H_2. These cases require either a single reactant undergoing a reaction of zero order or a surface which has only mobile active sites and permits one to treat the reactants as a two-dimensional gas. Furthermore, a third possibility, where the reaction takes place via two adsorbed molecules, must be eliminated as a separate case. Maatman has shown that such a Langmuir–Hinshelwood mechanism is indistinguishable from an Eley–Rideal mecha-

nism, if both reactants are adsorbed to a considerable degree and if the products of the rotational and translational partition functions of the two reactants differ significantly from each other. The reduction of NO by H_2 is restricted on both counts: the chemisorptions of H_2 and NO on Rh take place to an approximately equal extent (*6*), and the products of the partition functions differ by orders of magnitude.

These considerations leave two possible classes of reaction mechanisms for the reduction of NO by H_2. Case I [case 2 in Ref. (*26*)] encompasses as rate-determining step (a) the reaction between a molecule from the gas phase and an adsorbed molecule (Eley–Rideal mechanism), (b) the slow adsorption of a molecule in a system of one or two reactants, and (c) the reaction between two adsorbed molecules (Langmuir–Hinshelwood mechanism) under certain restrictions. Case II [case 4 in Ref. (*26*)] is described by the rapid adsorption of a reactant molecule, followed by dissociation of this molecule as the slow step.

The results of the site-density calculations for both cases are given in Table 4 for the two Rh phases. In case I, the calculated site densities on the samples with the two lower Rh concentrations exceed the measured densities by three orders of magnitude, while at the two higher Rh concentrations, the agreement between experimental and theoretical site density is remarkably good. In case II, the calculated site density refers to the concentration of bare dual sites at any instant. The dual site density is always within one or two orders of magnitude of the total number of active sites (*26*). Thus, in case II the calculated and measured site densities are in reasonable agreement for the catalyst at the lower Rh concentrations, but not for those catalysts at the higher concentrations.

Therefore, we deduce that the preferential formation of nitrous oxide over Rh at lower concentrations, which has been

TABLE 4

Comparison of Experimental and Theoretical Site Density

Rh loading (wt%)	Site density (per m^2)		
	Calculated		Measured Single sites
	Case I[a] Single sites	Case II[b] Dual sites	
0.34	0.8×10^{20}	3.3×10^{14}	1.3×10^{17}
1.89	3.3×10^{20}	1.3×10^{15}	7.3×10^{17}
5.51	1.8×10^{18}	7.2×10^{12}	1.5×10^{18}
12.40	1.9×10^{18}	7.4×10^{12}	1.5×10^{18}

[a] Case 2 in Ref. (*26*).
[b] Case 4 in Ref. (*26*).

also observed on other surfaces with a sparse coverage of active sites (*27*), cannot be explained by a mechanism in which the rate-controlling step involves a single surface site. The calculation suggests that the NO molecule must be dissociated on a dual site before it can react with another NO molecule, possibly from the gas phase, while the oxygen atom is removed from the surface by hydrogen. It is not unreasonable to assign the measured activation energy of 15 kcal/mol (Table 3) to this dissociation, as Winter (*28*) measured 14 kcal/mol for the dissociation of NO molecules adsorbed on Rh_2O_3.

Dissociation of NO is not the slow reaction step at higher Rh concentrations, as a comparison of the measured site density and that calculated for case II (Table 4) shows. Any of the three rate-determining steps listed under case I is possible here. Indications are that there are sufficient neighboring sites available to form a complex consisting of two NO molecules and two hydrogen atoms (*18*). Such a complex can produce N_2O by decomposition, or can be reduced further to nitrogen by additional hydrogen. Although the comparison of calculated and experimental site densities does not prove a certain reaction mechanism, it supports the idea that the rate-determining step changes when proceeding from a dilute catalyst, on which the active sites are dispersed in a two-dimensional

array, to a concentrated catalyst, where the active phase is present in three-dimensional particles.

CONCLUSIONS

At low Rh concentrations the catalytic activity of $Rh/\gamma\text{-}Al_2O_3$ catalysts increases in direct proportion to the Rh loading. This observation was made for (a) a reaction taking place under the reducing conditions of hydrogenolysis, where the active phase is in the form of a disperse, two-dimensional metallic phase; (b) the oxidation of *n*-butane, where the active catalyst is probably present as δ-phase Rh^{3+}; and (c) the NO reduction by H_2 under nearly stoichiometric conditions. In all three cases, the rate increase is linear within experimental error, shown by a uniform slope of 1.0 ± 0.2 of the reaction plots (Figs. 2, 3, and 5), until the Rh concentration reaches the saturation value 2.7 ± 0.3 $\mu mol/m^2$ on the $Rh/\gamma\text{-}Al_2O_3$ surface.

After the saturation concentration of the dispersed Rh phase has been reached, the proportionality between specific rate and surface Rh concentration is maintained for the oxidation of *n*-butane, but not for the reduction of nitric oxide by hydrogen and the hydrogenolysis of *n*-pentane. Changes in the reaction parameters and in the product distributions indicate strongly that the rate-determining step in the NO reduction and the reaction intermediate of *n*-pentane hydrogenolysis change as the Rh surface phase changes.

Supported catalysts on which relatively sharp changes take place from one surface aggregation state to another, as in the case of $Rh/\gamma\text{-}Al_2O_3$, can serve for the discrimination between demanding (structure sensitive) and facile (structure insensitive) reactions. Conversely, structure-sensitive reactions can be used to determine whether a supported catalyst contains predominantly highly dispersed metal (or metal oxide) or three-dimensional particles, which approach the catalytic behavior of non-supported catalysts. The data presented here show that on the same catalyst the change from a dispersed to a particulate phase can cause a decrease (*n*-pentane hydrogenolysis) or an increase (NO reduction by H_2) in specific activity.

ACKNOWLEDGMENTS

This work was carried out under the auspices of the Inter-Industry Emission Control Program which was a cooperative effort of Amoco Oil Company Atlantic Richfield Company, Ford Motor Company, Marathon Oil Company, Mitsubishi Motors Corporation (Japan), Mobil Oil Corporation, Nissan Motor Company, Ltd. (Japan), the Standard Oil Company of Ohio, and Toyota Motor Company Ltd. (Japan).

We thank Dr. M. Shelef for his interest during all phases of this work and, in particular, acknowledge his suggestions during the preparation of the manuscript.

REFERENCES

1. O'Reilly, D. E., and MacIver, D. S., *J. Phys. Chem.* **66**, 276 (1962).
2. Poole, C. P., and MacIver, D. S., *Advan. Catal.* **17**, 223 (1962).
3. Tomlinson, J. R., Keeling, R. O., Jr., Rymer, G. T., and Bridges, J. M., *Actes Due Deuxieme Cong. Int. Catal.*, Paris, 1960, p. 1831.
4. Yao, H. C., and Bettman M., *J. Catal.* **41**, 349 (1976).
5. Yao, H. C., and Shelef, M., *J. Catal.* **44**, 392 (1976).
6. Yao, H. C., Japar, S., and Shelef, M., *J. Catal.* **50**, 407 (1977).
7. Yao, H. C., and Shelef, M., "The Catalytic Chemistry of Nitrogen Oxides," pp. 45–59. Plenum, New York, 1975.
8. Yao, H. C., and Rothschild, W. G., *J. Chem. Phys.* **68**, 4774 (1978).
9. Corolleur, C., Corolleur, S., and Gault, F. G., *J. Catal.* **24**, 385 (1972).
10. Corolleur, C., Tomanova, D., and Gault, F. G., *J. Catal.* **24**, 401 (1972).
11. DeLaney, J. E., and Manogue, W. H., *In* "Proceedings, Fifth International Congress on Catalysis" (J. W. Hightower, Ed.), Vol. 1, p. 267. North-Holland, Amsterdam, 1973.
12. Ostermaier, J. J., Katzer, J. R., and Manogue, W. H., *J. Catal.* **33**, 457 (1974); **41**, 277 (1976).
13. Pusateri, R. J., Katzer, J. R., and Manogue, W. H., *AIChE J.* **20**, 219 (1974).
14. Boudart, M., Aldag, A. W., Ptak, L.D., and Benson, J. E., *J. Catal.* **11**, 35 (1968).

15. Yates, D. J. C., and Sinfelt, J. H., *J. Catal.* **8**, 348 (1967).
16. Dalla Betta, R. A., Piken, A. G., and Shelef, M., *J. Catal.* **35**, 54 (1974).
17. Yao, Y.-F. Yu, and Kummer, J. T., *J. Catal.* **46**, 388 (1977).
18. Otto, K., Shelef, M., and Kummer, J. T., *J. Phys. Chem.* **74**, 2690 (1970).
19. Yao, H. C., and Shelef, M., *J. Catal.* **56**, 12 (1979).
20. Leclercq, G., Leclercq, L., and Maurel, R., *J. Catal.* **50**, 87 (1977).
21. Ghorbel, A., Hoang-Van, C., and Teichner S. J., *J. Catal.* **30**, 298 (1973); **33**, 123 (1974).
22. Teichner, S. J., Mazabrard, A. R., Pajonk, G., Gardes, G. E. E., and Hoang-Van, C., *J. Colloid Interface Sci.* **58**, 88 (1977).
23. Darling, A. S., *In* "International Metallurgical Reviews" (U. S. Bristow, Ed.), Vol. 18, Review 175, p. 91 The Institute of Metals, London, and the American Society for Metals, Metals Park, Ohio, 1973.
24. Otto, K., and Shelef, M., *J. Phys. Chem.* **76**, 37 (1972).
25. Otto, K., and Shelef, M., *Z. Phys. Chem. NF* **85**, 308 (1973).
26. Maatman, R. W., *J. Catal.* **43**, 1 (1976).
27. Otto, K., unpublished data.
28. Winter, E. R. S., *J. Catal.* **22**, 158 (1971).